Nanocrystal formation in thermally oxidized and annealed a-Si:H films and SiO_xN_y films (x=0.17; y=0.07)

Sandeep Kohli,[*][a] Jeremy A. Theil[b], Rick D. Snyder[c], Patrick R. McCurdy
Christopher D. Rithner[a] and Peter K. Dorhout[a]
[a] Department of Chemistry, Colorado State University, Fort Collins CO-80523
[b] Agilent Technologies, MS 51L-GW, 5301 Stevens Creek Boulevard, Santa Clara, California 95051
[c] Agilent Technologies, MS-23, 4380 Zeigler Road, Fort Collins, Colorado 80525

ABSTRACT

Silicon nanocrystals have been prepared in thermally oxidized hydrogenated amorphous silicon (a-Si:H) and annealed silicon–rich oxynitride (SRON) films with [O/Si]=0.17, in the temperature range 400-800°C and 850-1150°C respectively. Glancing Angle X-ray Diffraction (GAXRD) measurements show the presence of silicon nanocrystals embedded in silicon oxide films. Warren-Averbach Analysis of GAXRD data indicates the presence of ~9nm silicon crystallites in a-Si:H films oxidized at 800°C. Room temperature photo-luminescence (PL) was observed from silicon nanocrystals embedded in oxidized a-Si:H films. Modeling the PL data indicates the presence of 6 nm silicon nanocrystals. This discrepancy is attributed to the columnar growth of silicon nanocrystals in thermally oxidized a-Si:H films. Silicon nanocrystals were not formed by thermal oxidation of SRON films under similar reaction conditions. However, silicon nanocrystals could be fabricated by annealing SRON films for 4 h in vacuum in the temperature ranges 850-1150°C. Silicon crystallite size remained constant (~4 nm) for films annealed below 1050°C and increased to 9 nm for films annealed at 1150°C. The presence of nitrogen played an important role in the silicon nanocrystal precipitation in SRON films. While the nanocrystal formation in a-Si:H films is due to oxidation and crystallization progressing simultaneously in the films, nanocrystal formation in SRON films is due to the high temperature precipitation of excess silicon in the film.

Keywords: nanocrystals, thin film a-Si:H, silicon-rich silicon oxide, oxidation, annealing

[*] skohli@lamar.colostate.edu; phone: 970 491-4076; fax: 970 491-1801

1. INTRODUCTION

Nanocrystals are a class of tunable materials whose electrical, chemical; optical and structural properties are determined by the size of the crystallite. Semiconductor[1-3] and metal[4-6] nanocrystals embedded in an oxide film are of great interest due to their ease of fabrication and application in light-emitting and memory devices. Although semiconductor nanocrystals of various elements and their compound structures have been fabricated, commercial applications involving electroluminescent materials that are compatible with integrated circuit technology may require nano-structures in the form of thin films that are compatible with current methods of silicon-based device fabrication. For example, bulk silicon cannot luminescence due to its indirect band gap; therefore cannot be used for photonic or electro-luminescent devices. However, silicon nanocrystals that are smaller than the exciton Bohr diameter of bulk silicon crystal (~10 nm) do have this ability because of quantum confinement effects.[7]

Porous Silicon (PS) is one example of a heterogeneous silicon nano-structure fabricated by electrochemical methods that also has the ability to luminescence efficiently. However, the mechanical and optical instability of PS has rendered this material unsuitable for the majority of device applications.[8] Light-emitting silicon nanocrystals embedded in a silicon oxide matrix are an ideal candidate for future electroluminescent and photonic devices because of their mechanical stability and their compatibility with current silicon-based device-manufacturing technology. Thermal oxidation and annealing are widely used techniques in the semiconductor industry. Hence, semiconductor nanocrystal formation by thermal oxidation and annealing of thin films offers the ability to create nanocrystals with large volume processing techniques, complementary with current silicon based device technology. Thermal oxidation has been used to fabricate germanium[9] and silicon[10] nanocrystals embedded in thin films while Si nanocrystal formation in the silicon-rich oxide films have been achieved by annealing the films in the temperature range 700-1100 ^{o}C for various annealing times.[11, 12] Nesbit had observed silicon nanocrystal growth in SiO_x ($0.72 \le x \le 1.4$) films annealed in the temperature range 700-1100°C.[11] In a recent article, Khomenkova[13] had investigated the luminescence properties of silicon nanocrystal in annealed Si-SiO_x co-sputtered systems with Si content varying from 67%-20%. They had found a maximum PL intensity for films with Si content 43-47%. For Si contents higher than 57%, the PL peak position for Si nanocrystals was found to be constant at ~1.4eV, increasing monotonically to 1.6eV for a Si content in the range 57-30%. No PL for

Si nanocrystals was observed for a Si content lower than 30%. Annealing the SiO_x with higher silicon content is likely to yield larger silicon nanocrystallites with higher volume fraction. However, the presence of nitrogen in the film modulates the growth of silicon nanocrystals in silicon rich oxide films, leading to the formation of small crystallites with a large volume fraction.[14, 15] Hence it is likely that nitrogen-doped silicon-rich oxide (or silicon rich-oxynitride) films with high silicon content are likely to exhibit small silicon nanocrystallites with a large volume fraction. In the present paper we report our results to fabricate silicon nanocrystals by thermal oxidation of a-Si:H films[16] and high-temperature vacuum annealing of SRON films with [O/Si]=0.17. Room temperature luminescence in the visible range from silicon nanocrystals had been observed in our earlier studies of a-Si:H films oxidized at 800°C.[16]

2. EXPERIMENTAL

Low temperature plasma enhanced chemical vapor deposition (PECVD)[17] was used to deposit 50 nm a-Si:H films on (100) silicon and silica substrates; 140 nm silicon-rich oxynitride (SRON) films on (100) silicon wafer with 500 nm of silicon oxide in between the silicon substrate and oxynitride film. Films deposited on silicon and silica wafers were placed in a cleaned and closed silica beaker that was preheated to 950 °C for 6 h before each oxidation cycle to remove any contaminants that could interfere with the oxidation process. The furnace was heated to the desired temperature and allowed to stabilize for 1h. Samples were heated at 400-800 °C for 1 h and allowed to cool in the furnace.

In addition to thermal oxidation, as described above, SRON films were also placed in vacuum-sealed fused silica ampoules of 12 mm inner diameter. The vacuum was better than 10^{-5} torr. The furnace was heated to the desired temperature and allowed to stabilize for 1h. Sealed ampoules were then placed in the furnace heated in the range 850-1150 °C for 4 h and allowed to cool in the furnace. It typically takes 3-4 h for the furnace to cool down to room temperature.

Glancing Angle X-ray Diffraction (GAXRD), X-ray Photoelectron Spectroscopy (XPS), Fourier Transform Infrared Spectroscopy (FTIR) were used to investigate the structural, chemical and vibrational properties of as-deposited

as well as oxidized and annealed films. The Warren-Averbach [18, 19] method was used for the estimation of crystallite size using Si(111) and (220) reflections at 28.44 and 47.30°.[20] Si (111) and (220) peaks were chosen for the estimation of the crystallite size due to the better signal-to-noise ratio. Standard Si [20] was used as a control and for estimation of the strain in our films. XPS survey measurements with a pass energy of 93.9 eV, step size 0.8 eV were performed using monochromatic $Al_{k\alpha}$ energy, 1486.6 eV X-ray source at a collection angle of 45°. Integrated peak area intensities under O1*s*, Si2*p* and N1*s* peaks were used for estimating the relative elemental composition of the films. The integrated peak area was normalized with respect to each core level atomic sensitivity factor. Scans for chemical state identification of the elements of a-Si:H were carried out with pass energy of 58.7 eV and a step size of 0.13 eV. Room temperature Photoluminescence results for oxidized a-Si:H film are also reported here. SRON film thickness was measured using X-ray Reflectivity (XRR) with a four-bounce monochromator on the incident beam side. The four-bounce monochromator was not used for XRR studies on the a-Si:H films. More details on our experimental procedures are provided elsewhere.[16, 21]

3. RESULTS

3.1 Thermally oxidized a-Si:H films

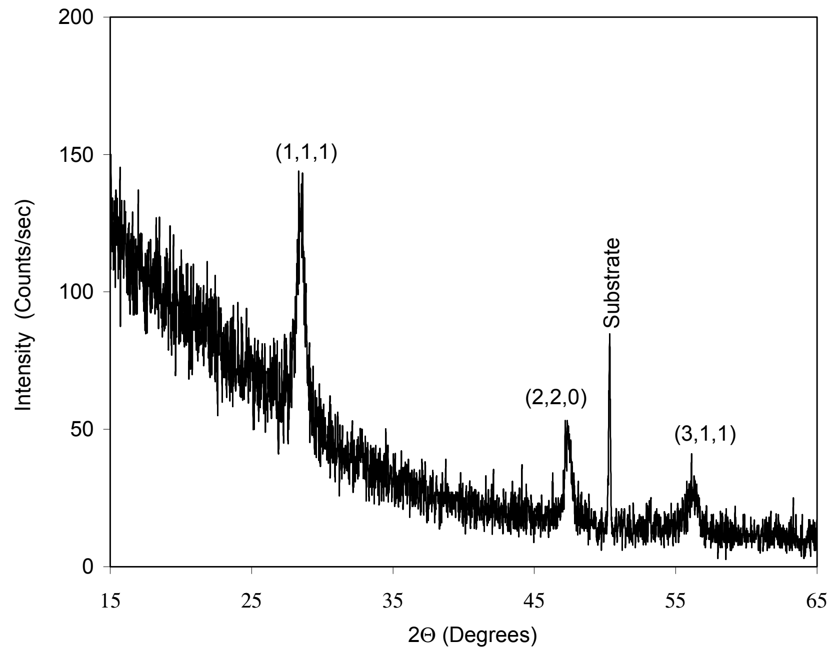

Figure 1. Glancing Angle X-ray Diffraction patterns for the a-Si:H films oxidized in air at 800°C. The Miller indices for the silicon peaks are also shown.

Fig 1 shows the GAXRD patterns for the a-Si:H films deposited on silicon substrate and oxidized at 800 ^{o}C at a fixed angle of incidence of 0.25^{o}. The XRD pattern for the film oxidized at 800°C showed the presence of silicon peaks with the preferred orientation along the (111) plane. The a-Si:H films deposited on the "silica" substrate and oxidized at 800 ^{o}C also showed the presence of crystalline Si features without the sharp peak around 50°. The XRD pattern of as-deposited a-Si:H films and films oxidized at 400 ^{o}C and 600 ^{o}C did not yield any crystalline features; thus these films were deemed amorphous. The average silicon crystallite size was found to be 9 ±1 nm. The RMS strain values of crystallites also showed exponential dependence on crystallite size, rapidly decreasing with increasing crystallite length.[16]

In the FTIR spectra of the as-deposited films,[16] Si-H and SiH_2 bands around 2000 and 2100 cm^{-1} respectively were observed.[16, 22] Oxidizing the film in air at 400°C led to the incomplete loss of silicon bound hydrogen, as Si-H absorption bands were still observed in this case. However, no absorption corresponding to silicon bound hydrogen vibrations were observed for the a-Si:H film oxidized at 600°C, indicating the complete evolution of hydrogen from the sample. The oxidation at 600°C also led to limited oxidation of the film as supported by the presence of an absorption band in the vicinity of 1075cm^{-1}. It was concluded from the peak analysis of the 1075 cm^{-1} band that it comprised two peaks centered at 1075 cm^{-1} and 1060 cm^{-1}. Since the the frequency of the Si-O(s) vibration is a function of x in SiO_x films,[23, 24] it was concluded that the peak at 1060 cm^{-1} corresponded to x=1.75 for a-SiO_x; thus the oxidation of the film generated stoichiometric and non-stoichiometric a-SiO_2.

The room temperature PL spectra for the a-Si:H film oxidized at 800 °C is shown in Fig 2. PL spectra show the presence of peaks around 1.6, 1.7, 1.9, 2.0 and 2.1eV. The PL of the a-Si:H film oxidized at 800 °C had been explained in terms of formation of a-SiO_X:H and silicon nanocrystals.[16] The peak at 1.7 eV was attributed to the localized-to-localized state transitions in amorphous silicon and silicon based alloys, while the peak at 2.1 eV were attributed to molecular-like (or defect-like) transitions. [23] The peak at 1.9 eV was possibly due to the non-bridging oxygen-hole center ($\equiv$Si-O$^{\cdot}$)[25] while the PL peak ~ 1.6eV is due to the formation of silicon nanocrystal.

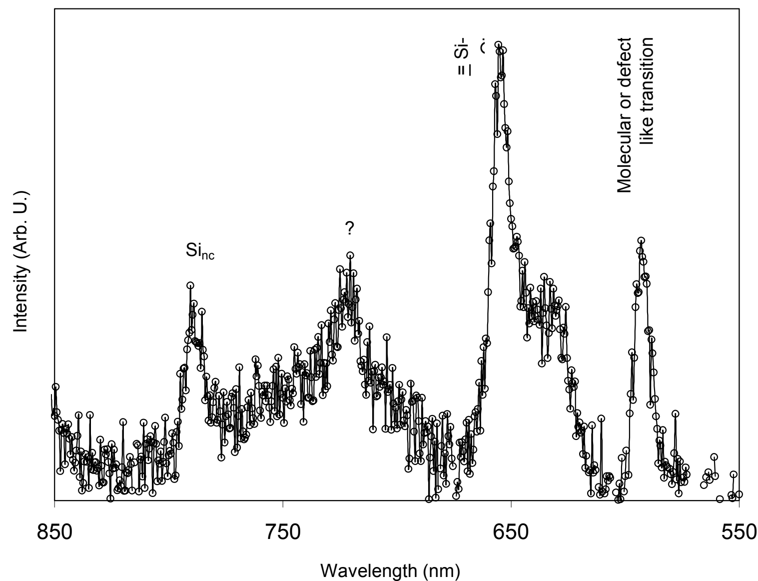

Figure 2 Room temperature PL spectra for the a-Si:H film oxidized at 800 ^{o}C. PL peak assignment is also shown.

3.2 Annealed silicon-rich oxynitride films

Figures 3-6 show the annealing characteristics of annealed SRON films. The XPS survey spectrum for the as-deposited sample after 5 min. of Ar^{+} ion sputtering to expose the underlying sample surface is shown in Figure 3. XPS analysis indicated that the as-deposited sample comprised Si, O and N with [O/Si]~0.17 and [N/Si] ~0.07. The presence of Ar in the spectra was attributed to the residual Ar present in the chamber after sputtering. Inset in the figure shows [O/Si] and [N/Si] ratio of as-deposited and annealed samples. As seen in the figure, the [O/Si] and [N/Si] ratio remained constant as a result of annealing.

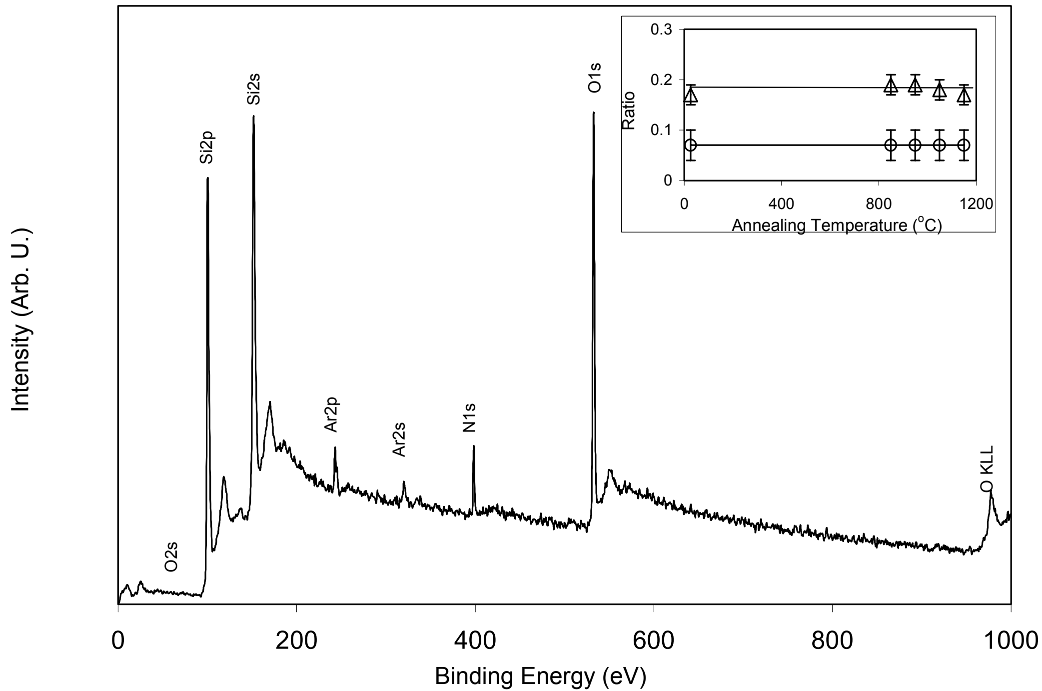

Figure 3. Survey XPS spectra for As-deposited SRON film after 5 min of Ar^{+} ion sputtering. Inset shows the [O/Si] (Δ) and [N/Si] (O) ratio as function of annealing temperature with the as-deposited film plotted at 27 ^{o}C.

Glancing Angle X-ray Diffraction patterns for the as-deposited and a sample annealed at 1150°C are shown in Figure 4. While the as-deposited sample was amorphous in nature, samples annealed at 850-1150 ^{o}C for 4h showed the

presence of silicon diffraction features. Measurements for estimating the silicon crystallite size were performed using the Si(111) and Si (220) peaks for 10 sec/step for an improved signal to the noise ratio. The estimated crystallite sizes were 5±2 nm, 4±2, 2±2 and 9 ±2 for samples annealed at 850 ^{o}C, 950°C, 1050°C and 1150°C respectively.

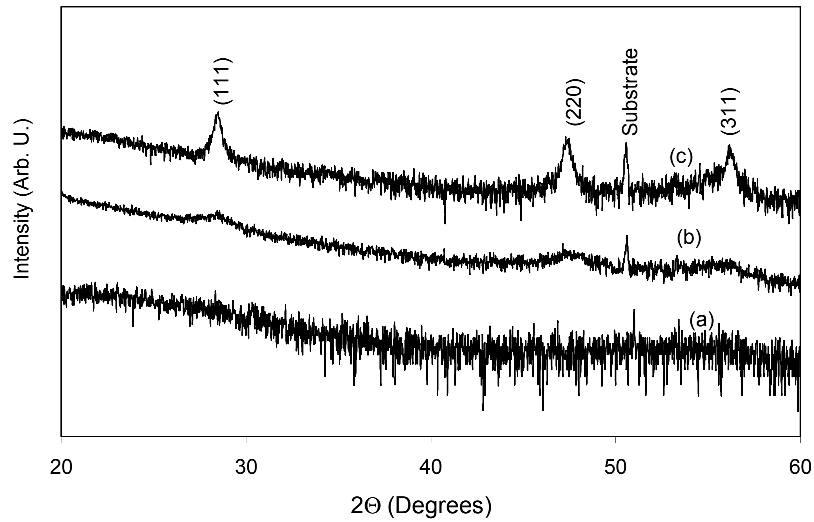

Figure 4. Glancing Angle X-ray Diffraction Pattern for as-deposited and annealed silicon-rich oxynitride films. Measurements were performed at an incident angel of 0.5^{o}. (a) As-deposited. (b) annealed at 850 ^{o}C and (c) annealed at 1150 ^{o}C.

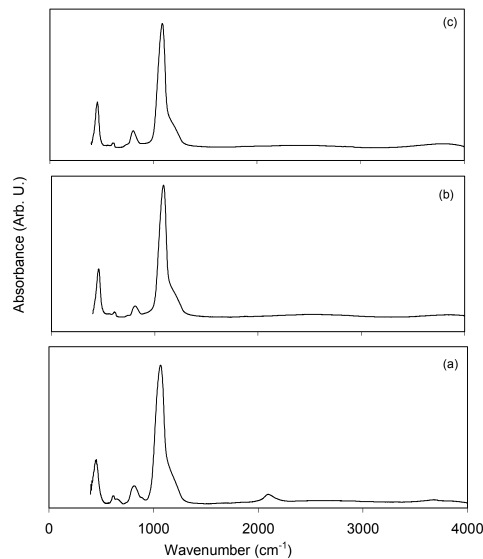

Figure 5. FTIR absorbance spectra of as-deposited and annealed SRON films. (a) As-deposited, (b) 850 ^{o}C and (c) 950 ^{o}C

Figure 5 shows the FTIR spectra of as-deposited and annealed SRON films. Spectra for as-deposited samples showed the presence of Si-H and Si-O (vibrations) around 2200[22] and 1080[23, 24] respectively. The Si-H peak was absent in annealed samples while Si-O peaks were shifted towards higher energies as compared to as-deposited films. In case of single-phase SiO_xN_y films the Si-O/Si-N peak varies from 850-1072 cm^{-1} for $0.26 \leq x \leq 2.0$ and $1.2 \geq y \geq 0$.[26] Detailed analysis of Si-H peak indicates the presence of a major band at 2104 cm^{-1} and two minor bands (<9%) around 2185 cm^{-1} and 2086 cm^{-1} respectively. However, the presence of a 500 nm SiO_2 film below the SRON film complicates the analysis of Si-O and Si-N peaks and is not attempted in this paper.

4. DISCUSSION

GAXRD results confirm the presence of ~ 9 nm silicon nanocrystals in a-Si:H films oxidized at 800 ^{o}C. These nanocrystals had preferred orientation along the Si (111) plane. As seen in the previously reported XPS results,[16] oxidation of film led to the formation of a Silicon oxide layer, with decreasing oxygen content towards the film-substrate interface. Analysis of IR peak around 1075 cm^{-1} indicated the presence of Stiochiometric and non-stiochiometric silicon oxide phases in films oxidized at temperatures ≥ 600°C. The PL peak around 1.6 eV was attributed to silicon nanocrystals and modeled based on one proposed by Chen[27] and extended by Trwoga[28]. This model assumed the radiative recombination of confined excitons to be the major contributor to the luminescence of nanocrystals and included the dependence of the oscillator strength on the cluster diameter. The modeled results gave an estimated crystallite size of ~5 nm.[16] The discrepancy in the estimation of crystallite size by the X-ray diffraction method and the PL analysis could be attributed to the columnar growth of the silicon nanocrystals, since the function representing the modeled oscillator strength applies to the smallest dimension of an irregular crystallite.[28] It seems that the low temperature PECVD process facilitated the growth of columnar morphology for the as-deposited films. As the film was heated to higher temperatures during annealing, hydrogen evolution from the film led to the formation of dangling bonds. As mentioned in our previous results, nanocrystal growth in thermally oxidized a-Si:H film occurred due to the

oxidation and crystallization of a-Si:H film proceeding simultaneously. Hence it is likely that varying the time and temperature conditions of the oxidation reaction occurring in the film could vary the crystallite size of the silicon nanocrystal.

For SRON films, nanocrystal growth is markedly different. The SRON films oxidized under similar reaction conditions did not yield any growth of Si nanocrystals. It is apparent that these conditions permit complete oxidation of the film. No attempt has been made at this stage to explore the nanocrystal growth in these films under different time-temperature reaction conditions.

GAXRD measurements on vacuum annealed SRON films indicate the formation of silicon nanocrystal. These nanocrystals did not exhibit any preferred orientation of planes. Crystallite size analysis indicated that, while the crystallite size for samples annealed at ≤ 1050 ^{o}C remained nearly constant at around 4 nm, samples annealed at 1150°C exhibited a larger crystallite size of 9±2 nm. The annealed samples showed lower strain values as a result of increased annealing temperatures. Results clearly indicated that while the increased annealing temperature ≤ 1050 ^{o}C did not cause increased crystallite size growth, it enabled strain relaxation due to separation of silicon nanocrystals and the oxide phase. However, annealing the sample at 1150 ^{o}C not only facilitated the increased crystallite size growth, it also enabled increased strain relaxation. The annealing temperature of SiO_2 lies around 1084 ^{o}C.[29] Hence, the increased crystallite size and strain relaxation can be attributed to the higher instability of the SRON films heated to 1150 ^{o}C, as compared to the SRON films heated at temperatures ≤ 1050 ^{o}C. It had been shown in the past that the presence of a nitrogen dopant strongly modulated the growth of Si nanocrystals in ion-implanted silicon-oxide [14] and silicon-rich oxide [15] films. In both the cases, the addition of nitrogen enabled the precipitation of silicon nanocrystals with reduced crystallite size as compared to undoped samples. Silicon nanocrystal formation in thermally annealed films is possible due to the breakage of Si-Si and Si-O bonds, leading to Si diffusion and phase separation. The bond strength of Si-Si and Si-N bonds at 298K are 325±7 and 470±15 kJmol^{-1} respectively.[30] Hence, it had been postulated that presence of a strong Si-N bond prevents the formation of Si-Si bonds that are necessary for coalescence of smaller Si particles to form larger crystallites. Thus, the presence of nitrogen enables the formation of a large number of silicon crystallites with small crystallite size.[14, 15] Based on their PL studies, Kachurian *et al.* [14] had noted that for fixed nitrogen content, the

crystallite size increased as the annealing temperature was raised from 900-1000°C. However, in our case, we observed the formation of nearly constant crystallite size as annealing temperature was varied from 850-1050°C. It must also be noted that crystallite size lower than 5nm, measured using Warren-Averbach method are subject to large uncertainties. More studies involving structural analysis by TEM are needed.

The peak frequency of Si-H, SiH_2 and SiH_3 IR bands of an amorphous solid have been correlated with the electronegativity of nearest neighbor bonding.[31] Joseph *et al.* had characterized the Si-H IR bands on the basis of this approach for their silicon-rich nitride and silicon-rich oxynitride films.[32] Based on these previous reports, we conclude that the major band at 2104 cm^{-1} correspond to an average bonding configuration of H-Si (O, Si, Si) while the bands around 2185 cm^{-1} and 2086 cm^{-1} corresponds to H-Si (O, O, Si) and H-Si (Si, Si, N) respectively. The elements in the parenthesis denote the nearest neighbors of Si bonded to H. Curve (a) in Figure 6 shows the difference in IR absorbance between the SRON sample annealed at 850 ^{o}C and the as-deposited sample. The sharp feature present in the difference curve is due to the shift of Si-O vibration band in the annealed SRON film towards higher frequency. However, this feature was minimized for the difference in IR absorbance between two annealed SRON samples, shown in the curve (b) in Fig 6. This clearly indicates the presence of Si with higher oxygen content in the annealed SRON film as compared to the as-deposited film. However, it must be noted that the IR spectra of the as-deposited and annealed samples includes overlapping features from the IR spectra of the SRON film and the 500 nm SiO_2 layer below it.

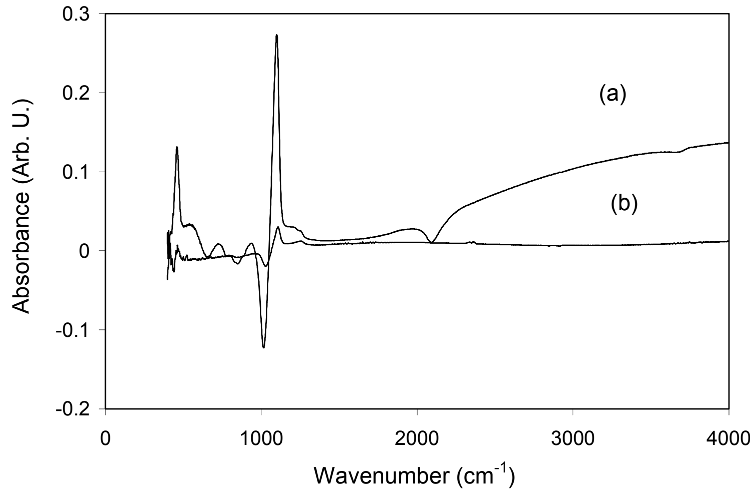

Figure 6. Difference in IR absorbance curves (a) IR $Curve_{850\ oC}$ –IR $Curve_{as\text{-}deposited\ curve}$ (b) IR $Curve_{950\ oC}$ –IR $Curve_{850oC}$

Annealed SiO_2 films are also likely to exhibit changes in their structural, optical and chemical properties. It had been seen in the past that annealing the SiO_2 films in vacuum causes the Si-O stretching band to shift towards higher energy.[33, 34] In order to deduce the shift due to SRON films only, the annealing effect of the underlying layer must be subtracted from the spectra. Annealing characteristics of 500 nm SiO_2, annealed under similar conditions, are currently being investigated. Preliminary results from these studies indicate that the Si-O stretching band shifts towards higher energies as the SRON sample is annealed at 850 ^oC. Increased annealing temperatures greater than 850 ^oC do not cause the Si-O band to shift towards higher energies. However, the XPS spectra do not indicate the presence of increased oxygen content in SRON films. This discrepancy is attributed to the high-temperature phase separation in SRON films where the material is separated into Si nanocrystals and a silicon-suboxide phase with higher oxygen content. This causes the Si-O vibration band to shift towards higher energy without the increased oxygen content tin the film. Similar effect has been seen in other SiO_x films with $0.7<x<1.3$. [35]

As described in our studies the Si nanocrystal formation in SRON films is due to the high temperature precipitation of silicon nanoparticles in SRON films. Thermal oxidation of these SRON films, under reaction conditions similar to the oxidation of a-Si:H film, led to the complete oxidation of the SRON, without the formation of silicon nanocrystals. The Presence of nitrogen strongly modulates the growth of nano-particles in annealed SRON films. Nearly

constant values of silicon crystallite size for SRON samples annealed at temperatures ≤ 1050 ^{o}C is attributed to the competing phenomena of Si / Si-O phase separation and Si-N bond formation. The annealing characteristics of the underlying layer must be taken into consideration for analyzing the FTIR spectra.

5. CONCLUSIONS

Silicon nanocrystals have been fabricated by the thermal oxidation of a-Si:H films in air. In our previous work, silicon nanocrystals could not be realized in SiO_xN_y with x= 0.17 under similar reaction conditions. However, silicon nano-particles could be achieved by annealing SRON films for 4h in vacuum, in the temperature range 850-1050 ^{o}C. Silicon crystallite size remained constant (~4 nm) for films annealed below 1050°C and increased to ~9 nm for the films annealed at 1150 ^{o}C. While the nanocrystal formation in a-Si:H films was due to oxidation and crystallization progressing simultaneously in the films, nanocrystal formation in SRON films is likely due to the high temperature phase separation of Si and Silicon-suboxide. In our case the crystallite size remained constant for films annealed at ≤1050 ^{o}C, increasing only when films were annealed at 1150 ^{o}C, although the number and size of crystallites were expected to increase with increased annealing temperature. It is likely that nitrogen played an important part in the silicon nano-particle formation in annealed SRON films.

ACKNOWLEDGEMENTS

The authors would like to acknowledge the financial support provided by the NSF instrument Grant Nos. NSF-CHE-9808024 and NSF-DMR-0076180.

REFERENCES

1. D. Nesheva and Z. Levi, "Nanocrystals of CdSe in thin film SiOx matrix," Semiconductor Science and Technology **12**(10), 1319-1322 (1997).
2. H. Nasu, K. Tsunetomo, Y. Tokumitsu, and Y. Osaka, "Semiconducting cadmium telluride microcrystalline-doped silicon dioxide glass thin films prepared by rf-sputtering," Japanese Journal of Applied Physics, Part 2: Letters **28**(5), L862-L864 (1989).
3. A. C. Rastogi, S. N. Sharma, and S. Kohli, "Size-dependent optical edge shifts and electrical conduction behaviour of RF magnetron sputtered CdTe nanocrystals:TiO2 composite thin films," Semiconductor Science and Technology **15**(11), 1011-1021 (2000).
4. T. Ung, L. M. Liz-Marzan, and P. Mulvaney, "Gold nanoparticle thin films," Colloids and Surfaces, A: Physicochemical and Engineering Aspects **202**(2-3), 119-126 (2002).
5. S. Deki, H. Y. Y. Ko, T. Fujita, K. Akamatsu, M. Mizuhata, and A. Kajinami, "Synthesis and microstructure of metal oxide thin films containing metal nanoparticles by liquid phase deposition (LPD) method," Eur. Phys. J. D **16**(1-3), 325-328 (2001).
6. D. M. Schaadt, E. T. Yu, S. Sankar, and A. E. Berkowitz, "Characterization and analysis of a novel hybrid magnetoelectronic device for magnetic field sensing," J. Vac. Sci. Technol., A **18**(4, Pt. 2), 1834-1837 (2000).
7. D. Kovalev, H. Heckler, G. Polisski, and F. Koch, "Optical properties of Si nanocrystals," Phys. Status Solidi B **215**(2), 871-932 (1999).
8. M. P. Stewart and J. M. Buriak, "Chemical and biological applications of porous silicon technology," Adv. Mater. (Weinheim, Fed. Repub. Ger.) **12**(12), 859-869 (2000).
9. Z. He, K. Chen, J. Xu, D. Feng, H. Han, and Z. Wang, "Luminescent Ge nanocrystallites embedded in a SiO2 films," Proceedings of SPIE-The International Society for Optical Engineering **3175**(Thin Film Physics and Applications), 37-41 (1998).
10. T. Maeda, E. Suzuki, I. Sakata, M. Yamanaka, and K. Ishii, "Electrical properties of Si nanocrystals embedded in an ultrathin oxide," Nanotechnology **10**(2), 127-131 (1999).
11. L. A. Nesbit, "Annealing characteristics of silicon-rich silicon dioxide films," Appl. Phys. Lett. **46**(1), 38-40 (1985).
12. L. p. You, C. L. Heng, S. Y. Ma, Z. C. Ma, W. H. Zong, Z. l. Wu, and G. G. Qin, "Precipitation and crystallization of nanometer Si clusters in annealed Si-rich SiO2 films," J. Cryst. Growth **212**(1/2), 109-114 (2000).
13. L. Khomenkova, N. Korsunska, V. Yukhimchuk, B. Jumayev, T. Torchynska, A. V. Hernandez, A. Many, Y. Goldstein, E. Savir, and J. Jedrzejewski, "Nature of visible luminescence and its excitation in Si-SiOx systems," J. Lumin. **102**, 705-711 (2003).
14. G. A. Kachurin, S. G. Yanovskaya, K. S. Zhuravlev, and M. O. Ruault, "The Role of Nitrogen in the Formation of Luminescent Silicon Nanoprecipitates during Heat Treatment of SiO2 Layers Implanted with Si+ ions," Semiconductors **35**(10), 1182-1186 (2001).
15. T. Ehara and S. Machida, "The effect of nitrogen doping on the structure of cluster or microcrystalline silicon embedded in thin SiO2 films," Thin Solid Films **346**(1,2), 275-279 (1999).
16. S. Kohli, J. A. Theil, R. D. Snyder, C. D. Rithner, and P. K. Dorhout, "Fabrication and characterization of silicon nanocrystals by thermal oxidation of a-Si:H films in air," J. Vac. Sci. Technol., B **21**(2), 719-728 (2003).
17. J. A. Theil, G. J. Kooi, and R. P. Varghese, "Chemical vapor deposition method for amorphous silicon and resulting film," 1164206 (2001).
18. B. E. Warren, "X-Ray Studies of Deformed Metals," Prog. Met. Phys. **8**, 147-202 (1959).
19. WIN-CRYSIZE Version 3.0, Crystallite Size and Microstrain, Sigma-C, München, Germany, 1996.
20. J. C. P. D. S.-I. C. D. D. Card No. 46-1025, (International Centre for DiffractionData, Newton Square, PA.).
21. S. Kohli, C. D. Rithner, and P. K. Dorhout, "X-ray characterization of annealed iridium films," J. Appl. Phys. **91**(3), 1149-1154 (2002).
22. J. Dian, J. Valenta, J. Hala, A. Poruba, P. Horvath, K. Luterova, I. Gregora, and I. Pelant, "Visible photoluminescence in hydrogenated amorphous silicon grown in microwave plasma from SiH4 strongly diluted with He," J. Appl. Phys. **86**(3), 1415-1419 (1999).
23. M. Zhu, Y. Han, R. B. Wehrspohn, C. Godet, R. Etemadi, and D. Ballutaud, "The origin of visible photoluminescence from silicon oxide thin films prepared by dual-plasma chemical vapor deposition," J. Appl. Phys. **83**(10), 5386-5393 (1998).
24. P. G. Pai, S. S. Chao, Y. Takagi, and G. Lucovsky, "Infrared spectroscopic study of silicon oxide (SiOx) films produced by plasma enhanced chemical vapor deposition," J. Vac. Sci. Technol., A **4**(3, Pt. 1), 689-694 (1986).
25. H. Nishikawa, E. Watanabe, D. Ito, Y. Sakurai, K. Nagasawa, and Y. Ohki, "Visible photoluminescence from Si clusters in .gamma.-irradiated amorphous SiO2," J. Appl. Phys. **80**(6), 3513-3517 (1996).
26. A. del Prado, I. Martil, M. Fernandez, and G. Gonzalez-Diaz, "Full composition range silicon oxynitride films deposited by ECR-PECVD at room temperature," Thin Solid Films **343-344**, 437-440 (1999).
27. C. Xiaoshuang, Z. Jijun, W. Guanghou, and S. Xuechu, "The effect of size distributions of Si nanoclusters on photoluminescence from ensembles of Si nanoclusters," Physics Letters A **212**(5), 285-289 (1996).

28. P. F. Trwoga, A. J. Kenyon, and C. W. Pitt, "Modeling the contribution of quantum confinement to luminescence from silicon nanoclusters," Journal of Applied Physics **83**(7), 3789-3794 (1998).
29. R. A. Lemons, M. A. Bosch, A. H. Dayem, J. K. Grogan, and P. M. Mankiewich, "Laser Crystallization of Si Films on Glass," Appl. Phys. Lett. **40**(6), 469-471 (1982).
30. , CRC Handbook of Chemistry and Physics (CRC Press, Boca Raton, Florida, USA), Vol. 81.
31. G. Lucovsky, "Chemical effects on the frequencies of silicon-hydrogen vibrations in amorphous solids," Solid State Commun. **29**(8), 571-576 (1979).
32. E. A. Joseph, C. Gross, H. Y. Liu, R. T. Laaksonen, and F. G. Celii, "Characterization of silicon-rich nitride and oxynitride films for polysilicon gate patterning. I. Physical, characterization," J. Vac. Sci. Technol., A **19**(5), 2483-2489 (2001).
33. W. K. Choi, C. K. Choo, K. K. Han, J. H. Chen, F. C. Loh, and K. L. Tan, "Densification of radio frequency sputtered silicon oxide films by rapid thermal annealing," J. Appl. Phys. **83**(4), 2308-2314 (1998).
34. D. B. Dimitrov, M. Beshkova, and R. Dafinova, "Influence of vacuum rapid thermal annealing on the properties of mu PCVD SiO2 and SiO2 center dot P2O5 films," Vacuum **58**(2-3), 485-489 (2000).
35. B. J. Hinds, F. Wang, D. M. Wolfe, C. L. Hinkle, and G. Lucovsky, "Study of SiOx decomposition kinetics and formation of Si nanocrystals in an SiO2 matrix," J. Non-Cryst. Solids **227-230**(Pt. A), 507-512 (1998).
~~1. D. Nesheva and Z. Levi, "Nanocrystals of CdSe in thin film SiOx matrix," Semiconductor Science and Technology **12**(10), 1319-1322 (1997).~~
~~2. H. Nasu, K. Tsunetomo, Y. Tokumitsu, and Y. Osaka, "Semiconducting cadmium telluride microcrystalline-doped silicon dioxide glass thin films prepared by rf-sputtering," Japanese Journal of Applied Physics, Part 2: Letters **28**(5), L862-L864 (1989).~~
~~3. A. C. Rastogi, S. N. Sharma, and S. Kohli, "Size-dependent optical edge shifts and electrical conduction behaviour of RF magnetron sputtered CdTe nanocrystals:TiO2 composite thin films," Semiconductor Science and Technology **15**(11), 1011-1021 (2000).~~
~~4. T. Ung, L. M. Liz-Marzan, and P. Mulvaney, "Gold nanoparticle thin films," Colloids and Surfaces, A: Physicochemical and Engineering Aspects **202**(2-3), 119-126 (2002).~~
~~5. S. Deki, H. Y. Y. Ko, T. Fujita, K. Akamatsu, M. Mizuhata, and A. Kajinami, "Synthesis and microstructure of metal oxide thin films containing metal nanoparticles by liquid phase deposition (LPD) method," Eur. Phys. J. D **16**(1-3), 325-328 (2001).~~
~~6. D. M. Schaadt, E. T. Yu, S. Sankar, and A. E. Berkowitz, "Characterization and analysis of a novel hybrid magnetoelectronic device for magnetic field sensing," J. Vac. Sci. Technol., A **18**(4, Pt. 2), 1834-1837 (2000).~~
~~7. D. Kovalev, H. Heckler, G. Polisski, and F. Koch, "Optical properties of Si nanocrystals," Phys. Status Solidi B **215**(2), 871-932 (1999).~~
~~8. M. P. Stewart and J. M. Buriak, "Chemical and biological applications of porous silicon technology," Adv. Mater. (Weinheim, Fed. Repub. Ger.) **12**(12), 859-869 (2000).~~
~~9. Z. He, K. Chen, J. Xu, D. Feng, H. Han, and Z. Wang, "Luminescent Ge nanocrystallites embedded in a SiO2 films," Proceedings of SPIE-The International Society for Optical Engineering **3175**(Thin Film Physics and Applications), 37-41 (1998).~~
~~10. T. Maeda, E. Suzuki, I. Sakata, M. Yamanaka, and K. Ishii, "Electrical properties of Si nanocrystals embedded in an ultrathin oxide," Nanotechnology **10**(2), 127-131 (1999).~~
~~11. L. A. Nesbit, "Annealing characteristics of silicon-rich silicon dioxide films," Appl. Phys. Lett. **46**(1), 38-40 (1985).~~
~~12. L. p. You, C. L. Heng, S. Y. Ma, Z. C. Ma, W. H. Zong, Z. l. Wu, and G. G. Qin, "Precipitation and crystallization of nanometer Si clusters in annealed Si-rich SiO2 films," J. Cryst. Growth **212**(1/2), 109-114 (2000).~~
~~13. L. Khomenkova, N. Korsunska, V. Yukhimchuk, B. Jumayev, T. Torchynska, A. V. Hernandez, A. Many, Y. Goldstein, E. Savir, and J. Jedrzejewski, "Nature of visible luminescence and its excitation in Si-SiOx systems," J. Lumin. **102**, 705-711 (2003).~~
~~14. G. A. Kachurin, S. G. Yanovskaya, K. S. Zhuravlev, and M. O. Ruault, "The Role of Nitrogen in the Formation of Luminescent Silicon Nanoprecipitates during Heat Treatment of SiO2 Layers Implanted with Si+ ions," Semiconductors **35**(10), 1182-1186 (2001).~~
~~15. T. Ehara and S. Machida, "The effect of nitrogen doping on the structure of cluster or microcrystalline silicon embedded in thin SiO2 films," Thin Solid Films **346**(1,2), 275-279 (1999).~~
~~16. S. Kohli, J. A. Theil, R. D. Snyder, C. D. Rithner, and P. K. Dorhout, "Fabrication and characterization of silicon nanocrystals by thermal oxidation of a-Si:H films in air," J. Vac. Sci. Technol., B **21**(2), 719-728 (2003).~~
~~17. J. A. Theil, G. J. Kooi, and R. P. Varghese, "Chemical vapor deposition method for amorphous silicon and resulting film," 1164206 (2001).~~
~~18. B. E. Warren, "X-Ray Studies of Deformed Metals," Prog. Met. Phys. **8**, 147-202 (1959).~~
~~19. WIN-CRYSIZE Version 3.0, Crystallite Size and Microstrain, Sigma-C, München, Germany, 1996.~~
~~20. J. C. P. D. S.-I. C. D. D. Card No. 46-1025, (International Centre for DiffractionData, Newton Square, PA.).~~
~~21. S. Kohli, C. D. Rithner, and P. K. Dorhout, "X-ray characterization of annealed iridium films," J. Appl. Phys. **91**(3), 1149-1154 (2002).~~

22. J. Dian, J. Valenta, J. Hala, A. Poruba, P. Horvath, K. Luterova, I. Gregora, and I. Pelant, "Visible photoluminescence in hydrogenated amorphous silicon grown in microwave plasma from SiH4 strongly diluted with He," J. Appl. Phys. **86**(3), 1415-1419 (1999).
23. M. Zhu, Y. Han, R. B. Wehrspohn, C. Godet, R. Etemadi, and D. Ballutaud, "The origin of visible photoluminescence from silicon oxide thin films prepared by dual-plasma chemical vapor deposition," J. Appl. Phys. **83**(10), 5386-5393 (1998).
24. P. G. Pai, S. S. Chao, Y. Takagi, and G. Lucovsky, "Infrared spectroscopic study of silicon oxide (SiOx) films produced by plasma enhanced chemical vapor deposition," J. Vac. Sci. Technol., A **4**(3, Pt. 1), 689-694 (1986).
25. H. Nishikawa, E. Watanabe, D. Ito, Y. Sakurai, K. Nagasawa, and Y. Ohki, "Visible photoluminescence from Si clusters in .gamma.-irradiated amorphous SiO2," J. Appl. Phys. **80**(6), 3513-3517 (1996).
26. A. del Prado, I. Martil, M. Fernandez, and G. Gonzalez-Diaz, "Full composition range silicon oxynitride films deposited by ECR-PECVD at room temperature," Thin Solid Films **343-344**, 437-440 (1999).
27. C. Xiaoshuang, Z. Jijun, W. Guanghou, and S. Xuechu, "The effect of size distributions of Si nanoclusters on photoluminescence from ensembles of Si nanoclusters," Physics Letters A **212**(5), 285-289 (1996).
28. P. F. Trwoga, A. J. Kenyon, and C. W. Pitt, "Modeling the contribution of quantum confinement to luminescence from silicon nanoclusters," Journal of Applied Physics **83**(7), 3789-3794 (1998).
29. R. A. Lemons, M. A. Bosch, A. H. Dayem, J. K. Grogan, and P. M. Mankiewich, "Laser Crystallization of Si Films on Glass," Appl. Phys. Lett. **40**(6), 469-471 (1982).
30. , CRC Handbook of Chemistry and Physics (CRC Press, Boca Raton, Florida, USA), Vol. 81.
31. G. Lucovsky, "Chemical effects on the frequencies of silicon-hydrogen vibrations in amorphous solids," Solid State Commun. **29**(8), 571-576 (1979).
32. E. A. Joseph, C. Gross, H. Y. Liu, R. T. Laaksonen, and F. G. Celii, "Characterization of silicon-rich nitride and oxynitride films for polysilicon gate patterning. I. Physical, characterization," J. Vac. Sci. Technol., A **19**(5), 2483-2489 (2001).
33. W. K. Choi, C. K. Choo, K. K. Han, J. H. Chen, F. C. Loh, and K. L. Tan, "Densification of radio frequency sputtered silicon oxide films by rapid thermal annealing," J. Appl. Phys. **83**(4), 2308-2314 (1998).
34. D. B. Dimitrov, M. Beshkova, and R. Dafinova, "Influence of vacuum rapid thermal annealing on the properties of mu PCVD SiO2 and SiO2 center dot P2O5 films," Vacuum **58**(2-3), 485-489 (2000).
35. B. J. Hinds, F. Wang, D. M. Wolfe, C. L. Hinkle, and G. Lucovsky, "Study of SiOx decomposition kinetics and formation of Si nanocrystals in an SiO2 matrix," J. Non-Cryst. Solids **227-230**(Pt. A), 507-512 (1998).